

1 Online Supplemental Information

2

### 3 **WITHIN-LOCUS INCOMPATIBILITIES: MODEL**

4 In the simplest possible scenario, the two new mutations arise at the same locus at the  
 5 same time, but in different patches. In this model, the ancestral allele is  $b$ , and the two new  
 6 alleles are  $a$  and  $A$ . The patch in which  $a$  arises is arbitrarily designated Patch 1, and the patch in  
 7 which  $A$  arises is designated Patch 2. Since we are interested in the scenario in which both alleles  
 8 are advantageous compared to ancestral allele  $b$ , but incompatible with each other, we have  $w_{AA}$   
 9  $= w_{Ab} > w_{aa} = w_{ab} > w_{bb} = 1 \geq w_{Aa}$  (where  $w_{xy}$  is the fitness of an individual with alleles  $x$  and  $y$  at  
 10 the locus of interest; see Table 1 in main text).

11 Allele frequencies were tracked as follows. If  $q_i$  is the frequency of allele  $a$  in patch  $i$  and  
 12  $p_i$  is the frequency of allele  $A$  in patch  $i$ , then the frequency of allele  $b$  in patch  $i$  is  $r_i = 1 - q_i - p_i$ ,  
 13 and the frequency of  $A$  in patch  $i$  in the next generation will be its proportional weighted fitness  
 14 (e.g., Graur & Li 2000, p. 42):

15

$$16 \quad \frac{p_i q_i w_{Aa} + p_i r_i w_{Ab} + p_i^2 w_{AA}}{2p_i q_i w_{Aa} + 2p_i r_i w_{Ab} + 2q_i r_i w_{ab} + p_i^2 w_{AA} + r_i^2 w_{bb} + q_i^2 w_{aa}}. \quad (1)$$

17

18 Similar equations were constructed for updating the frequencies of  $a$  and  $b$ . Other  
 19 parameters, including variation in  $q_{\text{thresh}}$  and  $t_{\text{contact}}$ , were as for the epistasis model (see main  
 20 text). Also as described for the epistasis model, two sets of simulation runs were conducted with  
 21 the same parameter value ranges for fitnesses,  $m$ ,  $q_{\text{thresh}}$ , and  $t_{\text{contact}}$ .

22

### 23 **WITHIN-LOCUS INCOMPATIBILITIES: RESULTS**

24 Using the same classification scheme as for the epistasis model discussed in the main  
 25 text, we found that some mutation-order divergence occurred under a range of conditions (online  
 26 figures S1-S3). However, as in the epistasis model, strong population divergence was unlikely  
 27 unless gene flow was absent or extremely low. Extreme M.O. and Moderate M.O. were never  
 28 observed at migration rates above 0.01 and consistently occurred only when  $m < 0.001$ .

29 Three factors other than gene flow strongly affected the probability of mutation-order  
 30 divergence. First, as the difference in selective advantage of the two new mutations decreased

31 (i.e., as the ratio  $w_{AA}/w_{aa}$  decreased toward unity), mutation-order divergence became more likely  
32 (online figures S1-S3). This was because large differences in relative fitness caused the most fit  
33 allele, *A*, to fix in both patches. Second, staggering the timing of origination of mutations  
34 affected the outcome, but its effect depended upon other parameters in the model. When the first  
35 mutation (allele *a*) originated slightly before the second, mutation-order divergence was  
36 promoted, for example being observed when differences in the selective advantage of new  
37 mutations were relatively large (and larger than possible for extreme M.O. in the case of  
38 simultaneous emergence of both mutations, compare online figure S3a to S3b and online figure  
39 S3d to S3e). In contrast, when the first mutation, *a*, originated long before the second mutation  
40 (i.e. was given a large ‘leg-up’), the less advantageous allele could actually spread between and  
41 even fix in both patches, sometimes preventing mutation-order divergence (online figures S2 and  
42 S3). In part, this was due to the second mutation, *A*, which is most advantageous on its own,  
43 often finding itself in a low fitness heterozygote (*Aa*). The latter effect could only be ameliorated  
44 by extremely low migration rates that prevented allele *a* from rising in frequency in Patch 2.  
45 Third, an initial period of allopatric divergence tended to promote mutation-order divergence  
46 (online figure S3). Fourth, hybrid fitness has some effects, but they were weak: as  $w_{Aa}$  decreased  
47 from 0.9 (moderate incompatibility) to 0.001 (nearly complete incompatibility), the size of the ‘*A*  
48 fixed’ region was slightly reduced (compare top and bottom rows of online figure S2) as it  
49 became harder for allele *A* to spread to fixation in both patches.

50

## 51 **DIFFERENCES BETWEEN WITHIN- AND BETWEEN-LOCUS MODELS**

52         These results of the two models were qualitatively, and largely quantitatively, very  
53 similar. The main difference between the single locus and epistasis models was that in the  
54 epistasis model Moderate M.O. was often observed at parameter values where Extreme M.O.  
55 was seen in the single locus model (e.g. figure 3 versus online figure S2). This difference is  
56 easily understood by noting the fact that in the epistasis model, the high fitness genotypes are  
57 those that include ancestral alleles (*AAbb* and *aaBB*). By contrast, in the single-locus model, each  
58 derived allele directly competes with the one ancestral allele, since all are at the same locus.  
59 Thus in the epistasis model, the preservation of ancestral alleles combined with migration makes  
60 our ‘Extreme M.O.’ criterion harder to achieve.

61

62

63 Figure legends for supplementary online figures

64

65 online figure S1. The effect of migration rate and relative fitnesses on mutation-order divergence  
66 in the single-locus model. The circles with dashed line show the frequency of allele *A* in Patch 2  
67 (in which allele *A* initially arose). Squares with solid line show the same for Patch 1 (in which  
68 allele *a* initially arose). Relative fitnesses, migration rate, and  $q_{\text{thresh}}$  all interact to determine  
69 which allele fixes and whether mutation-order divergence occurs. Extreme mutation-order  
70 divergence occurs in this figure when  $p_1 \approx 0$  ( $q_1 \approx 1$ ) and  $p_2 \approx 1$  ( $q_2 \approx 0$ ).

71

72 online figure S2. Outcomes of simulations in the single-locus model as influenced by migration  
73 rate, the ratio ( $w_{AA}/w_{aa}$ ) of fitnesses of the two favored alleles, the lag between when the two  
74 different mutations arise ( $q_{\text{thresh}}$ ), and the fitness of the genotype with the two incompatible  
75 alleles ( $w_{Aa}$ ). Each panel represents outcomes from 10,000 simulations for varying combinations  
76 of the fitness ratio ( $w_{AA}/w_{aa}$ ) and the migration rate. Panel (e) shows the meaning of the different  
77 degrees of shading for all six panels. See main text for definitions of outcomes and abbreviations.

78

79 online figure S3. The role of a period of  $t_{\text{contact}}$  generations of allopatric divergence on the  
80 outcome of mutation-order divergence in the single-locus model. Shading is as for online figure  
81 S2. Top row: parameter values as in online figure S2a; bottom row: parameters values as for  
82 online figure 2f.

83

84 online figure S4. The role of extended periods of allopatric divergence in the epistasis model.  
85 Top row: parameter values from figure 3a (main text); bottom row: parameters values as figure  
86 3f (main text). Details are as for figure 4 in the main text.

87

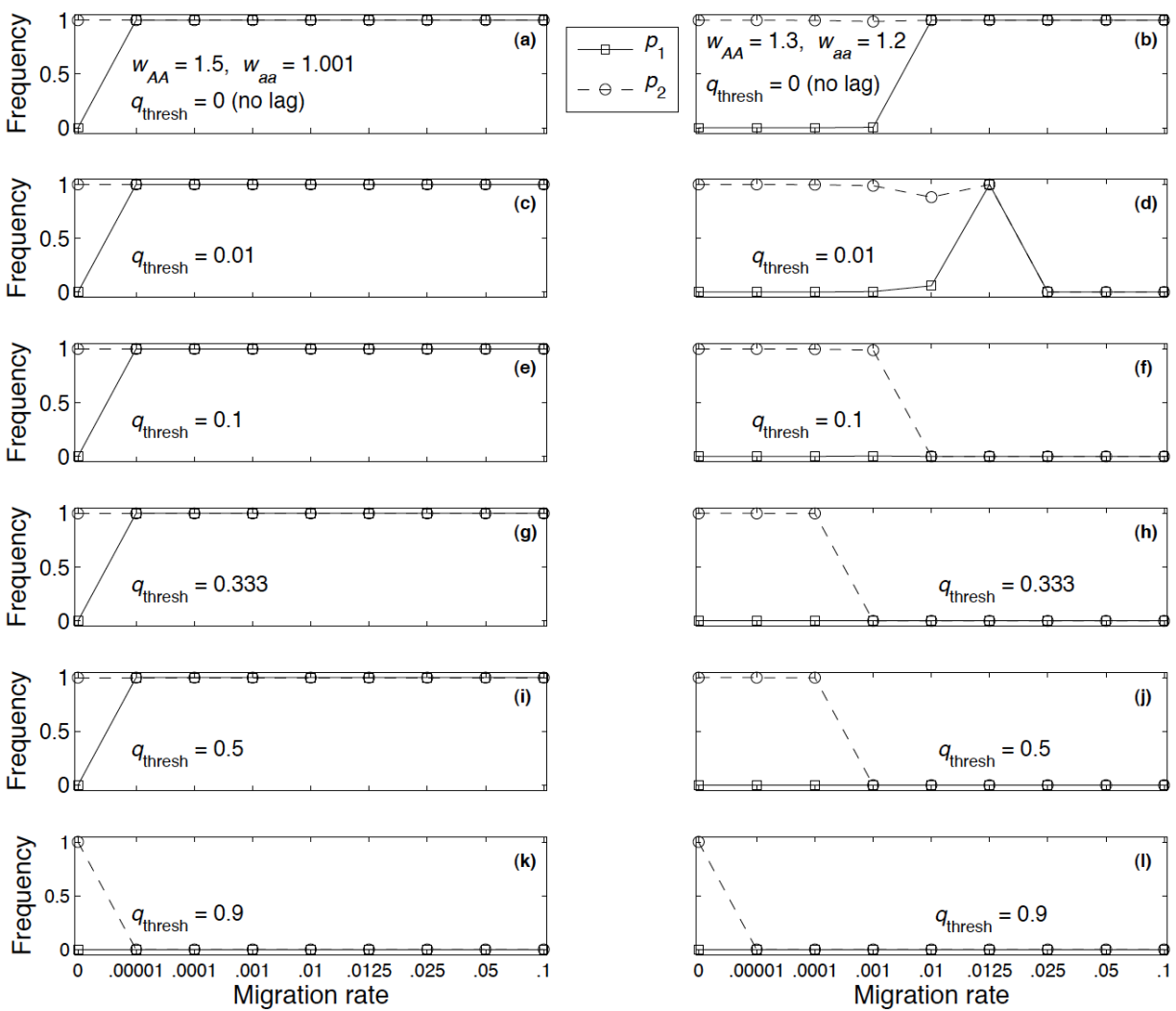
88 online figure S5. The effects of a range of parameter values for hybrid fitness and  $q_{\text{thresh}}$  for 30  
89 generations of allopatric divergence in the epistasis model. For comparison,  $q_{\text{thresh}}$  and  $t_{\text{contact}}$  take  
90 the same values here as in the six panels of figure 3 of main text.

91

92

93 online figure S1

94



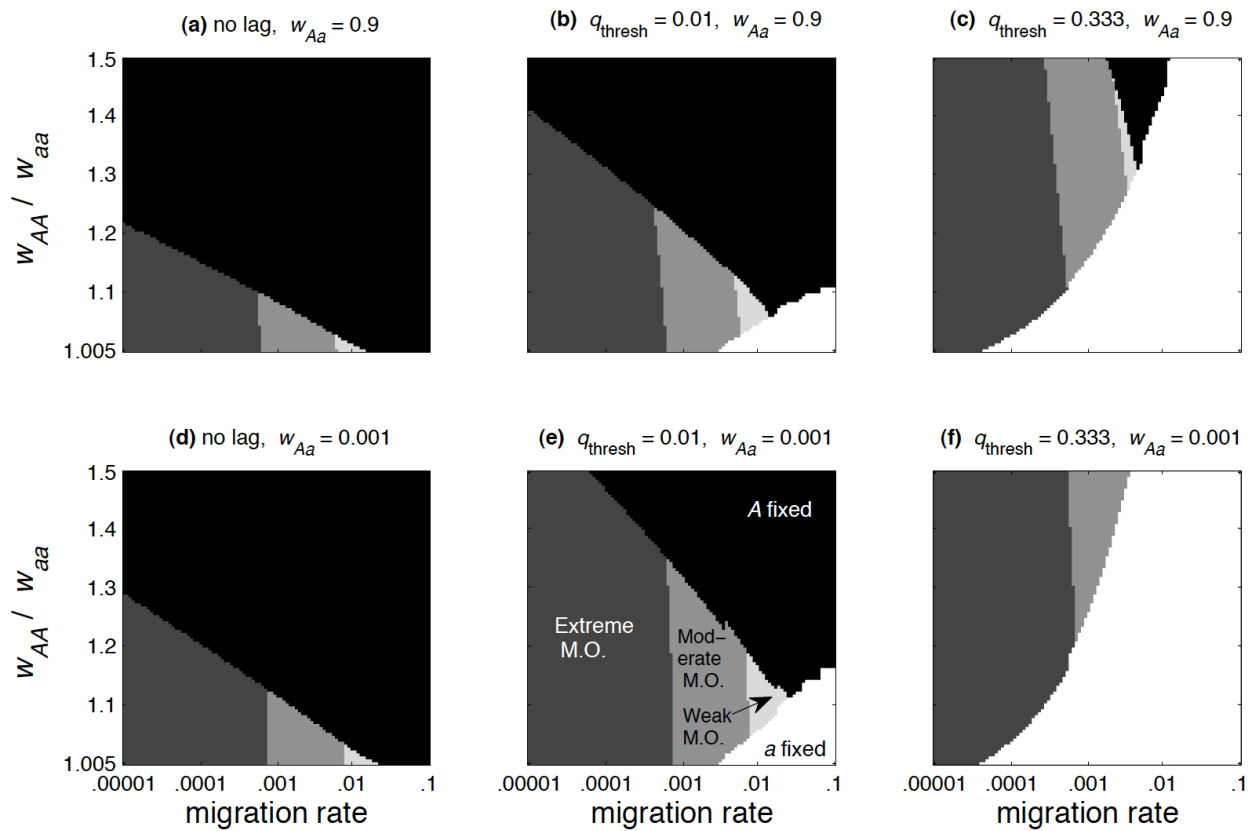
95

96

97

98 online figure S2

99



100

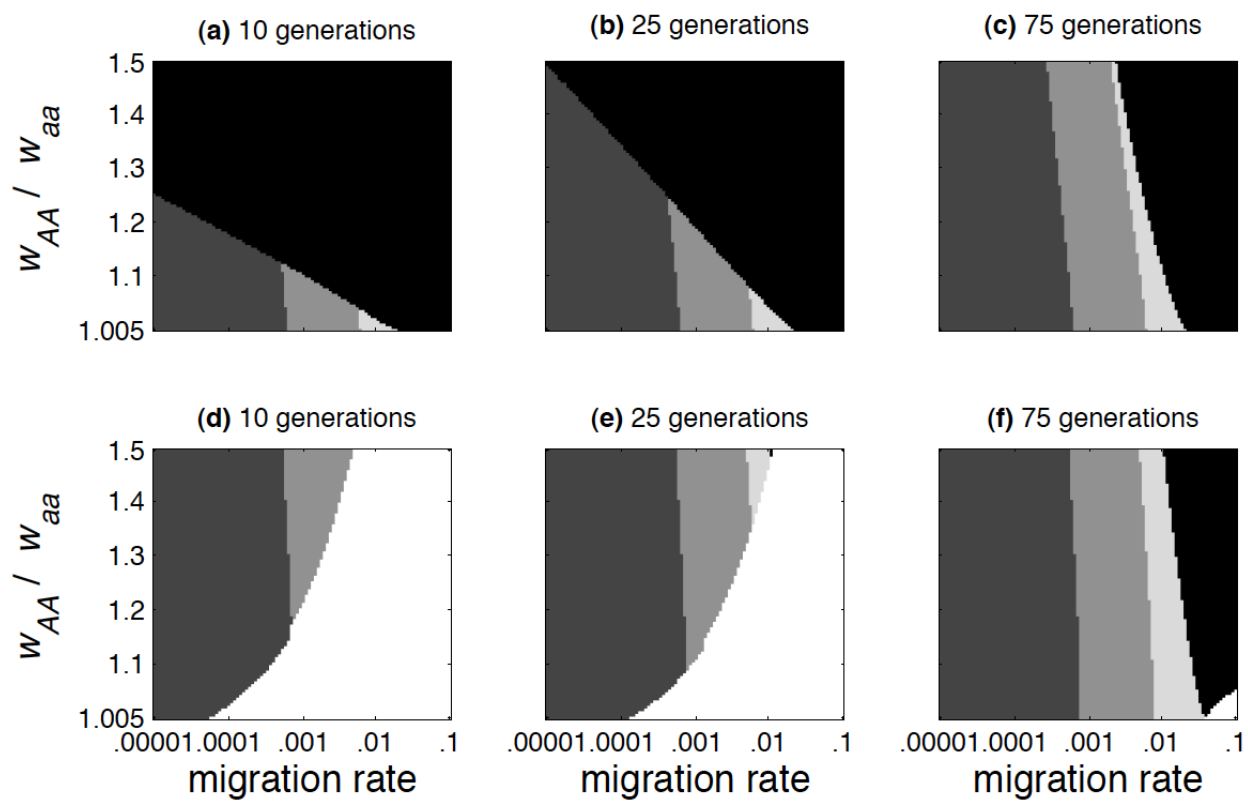
101

102

103 online figure S3

104

105



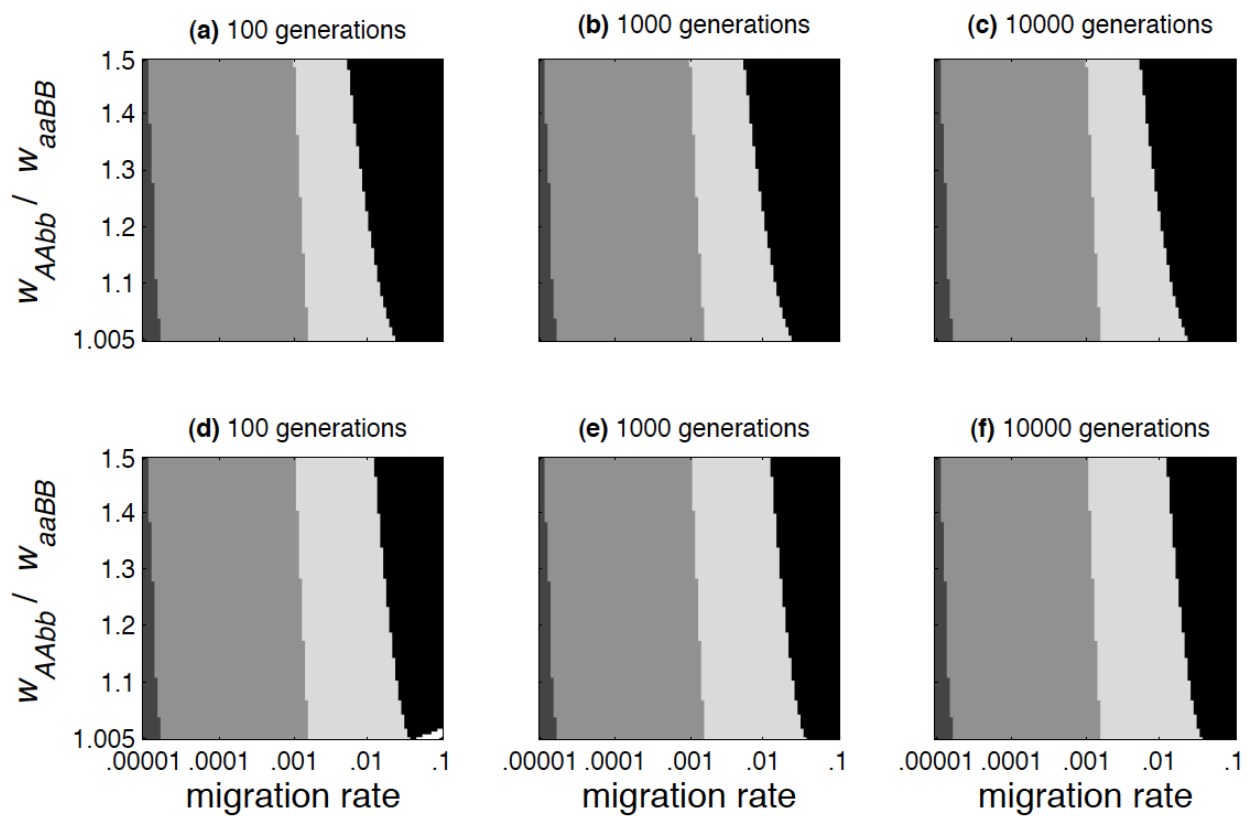
106

107

108

109 online figure S4

110



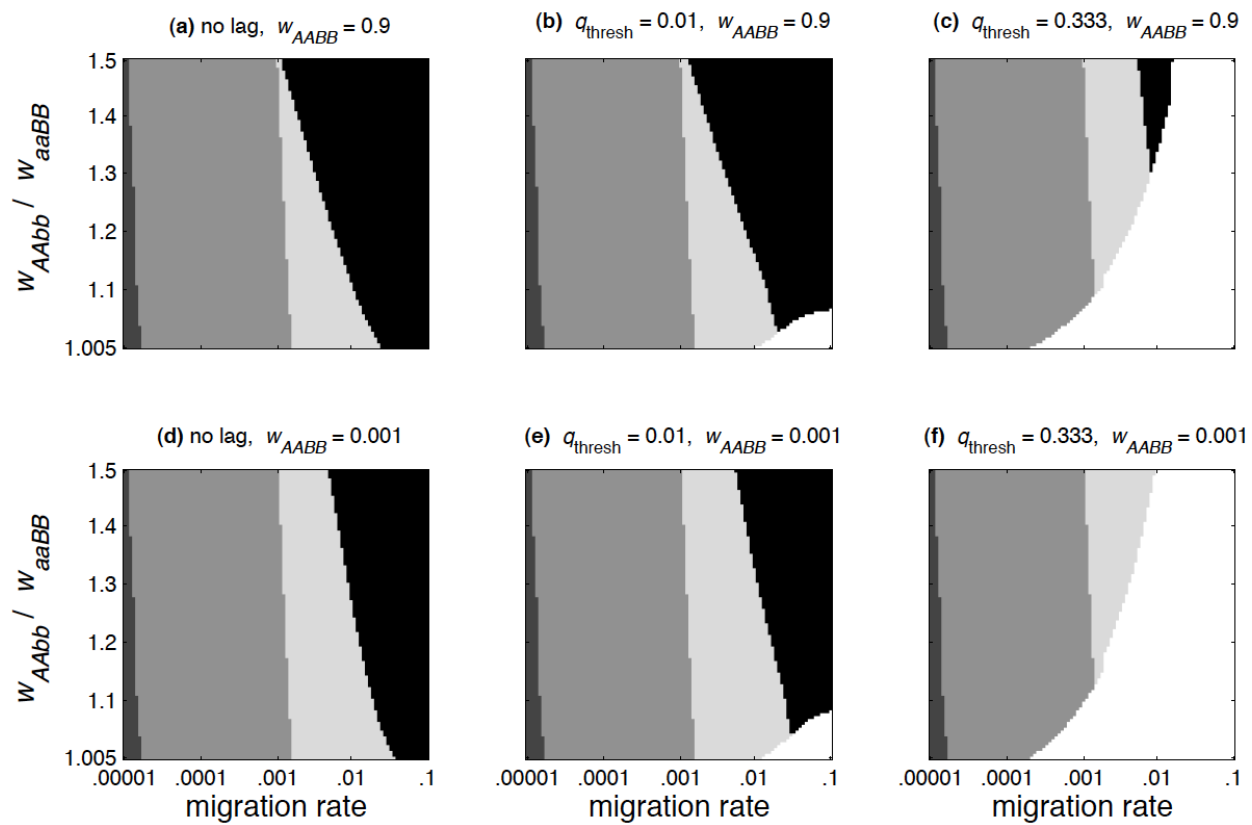
111

112

113

114 online figure S5

115



116

117

118